Nuclear Science and Techniques **24** (2013) 030503

Magnetic rotation in Rubidium-84

SHEN Shuifa[1,2,3,4,*] HAN Guangbing[5] WEN Shuxian[6] YAN Yupeng[2,3]
WU Xiaoguang[6] ZHU Lihua[7] HE Chuangye[6] LI Guangsheng[6]

[1]*Institute of Nuclear Energy Safety Technology, Chinese Academy of Sciences, Hefei 230031, Anhui, China*

[2]*School of Physics, Suranaree University of Technology, Nakhon Ratchasima 30000, Thailand*

[3]*Thailand Center of Excellence in Physics (ThEP), Commission on Higher Education, 328 Si Ayutthaya Road, Ratchathewi, Bangkok 10400, Thailand*

[4]*State Key Laboratory of Nuclear Physics and Technology (Peking University), Beijing 100871, China*

[5]*School of Physics, Shandong University, Jinan 250100, China*

[6]*China Institute of Atomic Energy, P. O. Box 275(10), Beijing 102413, China*

[7]*School of Physics and Nuclear Energy Engineering, Beihang University, Beijing 100191, China*

Abstract High-spin states in ^{84}Rb have been studied by using the ^{70}Zn(^{18}O, p3n)^{84}Rb reaction at beam energy of 75 MeV. Three regular magnetic dipole bands including strong M1 and weak E2 transitions have been observed in this nucleus which shows the characteristic feature of magnetic rotation. These bands are interpreted in the projected shell model for the first time on the basis of the four-quasiparticle configuration of the type $\pi(\mathrm{fp})\otimes\pi(\mathrm{g}_{9/2}^2)\otimes\nu(\mathrm{g}_{9/2})$. It is shown that the calculated sequence lies roughly in the same energy range as the experimental one but the interval between neighboring levels is larger than the corresponding experimental value. We believe that a 4-quasiparticle band crossing with the 2-quasiparticle band will depress the energies of the states.

Key words In-beam γ-spectroscopy, Magnetic dipole band, Projected shell model

1 Introduction

Magnetic rotation, a novel kind of nuclear rotation, has attracted a great interest in recent years. The levels of rotation bands are linked by strong magnetic dipole (M1) transitions whereas crossover electric quadrupole (E2) transitions are very weak. The ratios of the transition probabilities B(M1)/B(E2) are large. This magnetic character of the rotation is demonstrated by the ratios of transition probability B(M1)/B(E2) for each level in the band.

Experimental evidence of magnetic rotational bands is the presence of a greater intensity of ΔI=1 M1 transition between neighboring levels within one band in some nuclei with small deformation. These M1 transitions differ from the ones usually observed in high-spin states. At first, the energies of these transitions are very regular, that is, there doesn't exist signature splitting. It is very similar to high-K rotational band in nuclei with large deformation. Secondly, their magnetic dipole reduced transition probability B(M1) values are greatly enhanced, can up to several μ_N^2 units. Magnetic dipole and electric quadrupole reduced transition probability ratio B(M1)/B(E2) is very large. E2 transition within the band is very weak or can not be observed, this is different from the high-K band in a well deformed nucleus, which indicates that the deformation corresponding to this band is very small. Moreover, the ratio of the dynamic moment of inertia $J^{(2)}$ to electric quadrupole reduced transition probability B(E2) is larger than that of the normal deformation band and superdeformed band, it can be as large as 10 times more.

Supported by Suranaree University of Technology (No. 15/2553), Major State Basic Research Development Program in China (No.2007CB815003), National Natural Science Foundation of China (Nos.10975190, 11065001, 10975019, 10675170, and 61067001) and Foundation of the Education Department of Jiangxi Province (No.GJJ12372)

* Corresponding author. *E-mail address:* shuifa.shen@fds.org.cn

Received date: 2013-04-01

In recent years, the study of magnetic rotational band has been given great attention, either in theory or in experiments. At first, in previous years, magnetic rotational bands have been found in some nuclei in Pb region, e.g. in ^{199}Pb, ^{200}Pb, etc., in ^{139}Sm around A~140 mass region, in ^{110}Cd and ^{105}Sn around A~110 region, and in ^{82}Rb[1] and ^{84}Rb[2-4] around A~80 mass region etc. From the theoretical side, a different type of shell model calculations as well as relativistic mean–field (RMF) descriptions for the shears band mechanism in ^{84}Rb have been accomplished in this mass region about ten years ago[3,5], and its adjacent nucleus ^{82}Rb was also studied using the complex Excited Vampir approach[6]. This work focuses on the magnetic dipole band in ^{84}Rb and complements the preceding publication[7].

2 Assignment of magnetic dipole band in ^{84}Rb

High-spin states in ^{84}Rb are studied by the heavy ion fusion-evaporation reaction ^{70}Zn(^{18}O, p3n)^{84}Rb using the ^{18}O beam provided by the HI-13 tandem accelerator at China Institute of Atomic Energy (CIAE). Details of the experimental procedure and results were published recently in Ref.[7], where the negative-parity bands were extended greatly from the previous (6^-) up to the highest (17^-) and the spins and parities of these levels were tentatively assigned based on γ-γ directional correlations of oriented states (DCO) intensity ratios[8] and previous works. The γ-coincidence data were analyzed with the Radware software package[9]. In the present work we concentrate on the most interesting feature, the sudden development of regular magnetic dipole band at excitation energy around 3 MeV[7]. Note that the difference about the first M1 band (denoted as band C) between our work and the one by Schnare *et al.*[2] is one spin unit.

Among the three bands (denoted as bands C, D and E), band C is assigned as a magnetic rotational band at first. It consists of seven strong M1 transitions of 325, 444, 546, 655, 721, 765, and 874 keV on top of the I^{π}=(10^-) level at E_x=3.339 MeV. The dipole character of the transitions has been proven by the γ-γ directional correlations of oriented states (DCO) intensity ratios and the multipolarity M1 is suggested by the analogy to multiparticle excitations in neighboring nuclei. From its Routhian, it can be found that there does not exist signature splitting. The ratios of transition probabilities B(M1)/B(E2) are extracted. The error of these ratios is relatively large because the E2 transition is very weak, but the trend of the ratios can be given. The above experimental facts show that this band has a rotating magnetic characteristic. No E2 crossover transition is observed in bands of D and E, which are also identified as magnetic rotational bands.

3 Calculations in the framework of projected shell model

These magnetic dipole bands (the so-called shear bands) were normally described in the tilted-axis-cranking (TAC) model[10]. An interesting question is whether the shell-model calculations can describe the regular M1 band discussed above. In the present work, we try to describe the regular negative-parity M1 bands in ^{84}Rb within the projected shell model (PSM) for the first time on the basis of the lowest-lying four-quasiparticle (4qp) configuration with negative-parity $\pi(\mathrm{fp})\otimes\pi(\mathrm{g}_{9/2}^2)\otimes\nu(\mathrm{g}_{9/2})$, which is adopted from Ref.[2]. In recent years, the PSM has become quite successful in describing a broad range of properties of deformed nuclei in various regions of the nuclear Periodic Table. The most striking aspect of this model is its ability to describe finer details of high-spin spectroscopy data with simple physical pictures[11]. In this work, to study the magnetic dipole band, we apply this model to the representative nucleus ^{84}Rb. The PSM[12-15] employed in this work is a microscopic theory, which solves many-nucleon systems fully quantum mechanically. The ansatz for the angular-momentum-projected wave function is given by:

$$|IM\rangle = \sum_k f_k \hat{P}^I_{MK_k} |\varphi_k\rangle \qquad (1)$$

where k labels the basis states, and $\hat{P}^I_{MK}$ is the angular-momentum projection operator which is explicitly given in Ref.[12]. Acting on an intrinsic state $|\varphi_k\rangle$, the operator $\hat{P}^I_{MK}$ generates states of good angular momentum, and thus restores the necessary rotational symmetry violated in the

deformed mean field. The new shell model basis is constructed the way in which the Hamiltonian is diagonalized. The shell model basis taken in the present work is as follows:

$$\hat{P}^{I}_{MK}\left|\varphi_k\right\rangle \tag{2}$$

The basis states $\left|\varphi_k\right\rangle$ are spanned by the set

$$\left\{a_n^{+}a_p^{+}\left|0\right\rangle\right\} \tag{3}$$

for doubly odd nuclei, where $\left|0\right\rangle$ denotes the quasiparticle vacuum state and $a_n^{+}(a_p^{+})$ is the neutron (proton) quasiparticle creation operator for this vacuum, and the index n(p) runs over selected neutron (proton) quasiparticle states and k in Eq.(1) runs over the configuration of Eq.(3). The vacuum is obtained by diagonalizing a deformed Nilsson Hamiltonian[16] followed by a BCS calculation. In our calculations, we use three major shells, i.e., N = 2, 3, and 4 for neutrons (protons) as the configuration space.

In this work, we use the Hamiltonian[15]:

$$\hat{H}=\hat{H}_0-\frac{1}{2}\chi\sum_{\mu}\hat{Q}^{+}_{\mu}\hat{Q}_{\mu}-G_M\hat{P}^{+}\hat{P}-G_Q\sum_{\mu}\hat{P}^{+}_{\mu}\hat{P}_{\mu} \tag{4}$$

where $\hat{H}_0$ is the spherical single-particle shell model Hamiltonian, $\hat{Q}_{\mu}$ is the quadrupole moment operator, $\hat{P}$ and $\hat{P}_{\mu}$ are the monopole pairing operator and the quadrupole pairing operator, respectively. Though the theory itself is not bound to any particular form of Hamiltonian, the advantage of using such a separable-force Hamiltonian is that the role of each interaction is well known and, therefore, the interpretation of the numerical result becomes easier. The interaction strengths are determined as follows: the strength of the quadrupole-quadrupole interaction χ is adjusted by the self-consistent relation such that the input quadrupole deformation ε_2 and the one resulting from the HFB (Hartree-Fock-Bogolyubov) procedure coincide with each other[15]. The monopole pairing strength constant is adjusted to give the known energy gap:

$$G_M=[20.12\mp 13.13\frac{N-Z}{A}]\cdot A^{-1} \tag{5}$$

where "–" is for neutrons and "+" for protons. Finally, the quadrupole pairing strength G_Q is simply assumed to be proportional to G_M:

$$(\frac{G_Q}{G_M})_n=(\frac{G_Q}{G_M})_p=\gamma \tag{6}$$

The proportionality constant γ is chosen as 0.20 for all the bands calculated in the present work.

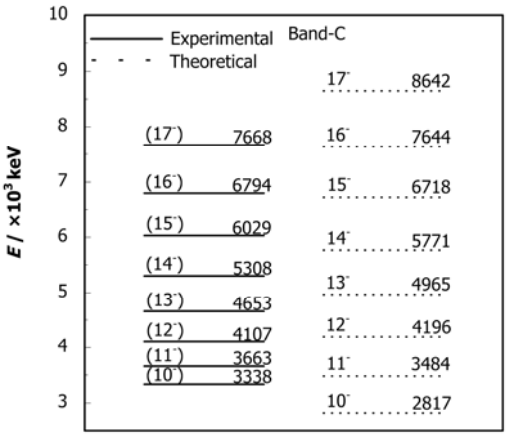

Fig.1 Comparison of calculated level energies with experimental results in the negative-parity M1 band denoted by band-C in ^{84}Rb.

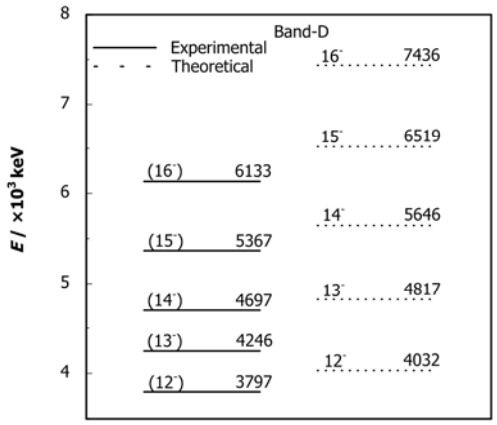

Fig.2 Comparison of calculated level energies with experimental results in the negative-parity M1 band denoted by band-D in ^{84}Rb.

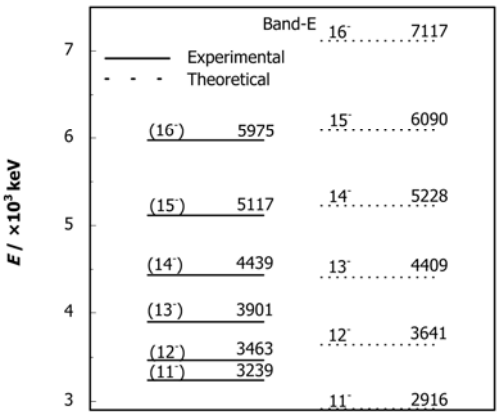

Fig.3 Comparison of calculated level energies with experimental results in the negative-parity M1 band denoted by band-E in ^{84}Rb.

In the calculations performed by Schnare *et al.*[2-4], the lowest-lying four-quasiparticle (4qp) configuration for Z=37 and N=47 turns out to be $\pi(\mathrm{fp})\otimes\pi(\mathrm{g}_{9/2}^2)\otimes\nu(\mathrm{g}_{9/2})$. This configuration has a negative parity which is consistent with our experimental findings. The "shears" mechanism is generated by two protons in the $g_{9/2}$ orbital and one unpaired $g_{9/2}$ neutron. In analogy to the study of the negative-parity yrast band in this nucleus which has been performed in our recently published work[7], we construct the configuration space in the magnetic dipole band calculations for ^{84}Rb by selecting the qp states close to the Fermi energy in the N=4 (N=3) major shell for neutrons (protons), that is, the K=7/2 orbital of the $g_{9/2}$ subshell (all orbitals of $p_{3/2}$ and $f_{5/2}$ subshells) to form multi-qp states. The quadrupole deformation parameter ε_2 =0.14 is adopted from Ref.[2] and the hexadecapole deformation parameter ε_4 =0.007 is taken from the compilation of Möller *et al.*[17]. Level energies calculated for the obtained level sequence are presented in Figs.1, 2 and 3, respectively, and compared with experimental results taken from our work (see Fig.2 of Ref.[7]). It is found from Figs.1, 2 and 3 that the order of the experimental states is well reproduced and the calculations predict roughly the energy range of the experimental M1 band. However, it is seen from Fig.1 that the calculated 12^- to 17^- states lie above the experimental ones in contrast to the low states with spins 10^- and 11^-. This may stem from that the two-quasiparticle (2qp) configuration $\pi(\mathrm{fp})\otimes\nu(\mathrm{g}_{9/2})$ is adopted in our calculations instead of the four-quasiparticle (4qp) configuration $\pi(\mathrm{fp})\otimes\pi(\mathrm{g}_{9/2}^2)\otimes\nu(\mathrm{g}_{9/2})$, that is, the alignment of a pair of $g_{9/2}$ protons has not been considered yet. The alignment of a pair of $g_{9/2}$ protons will lower the level energies. On the other hand, it is needed to include the triaxial deformation parameter γ[2] and thus will also lower the level energies[18].

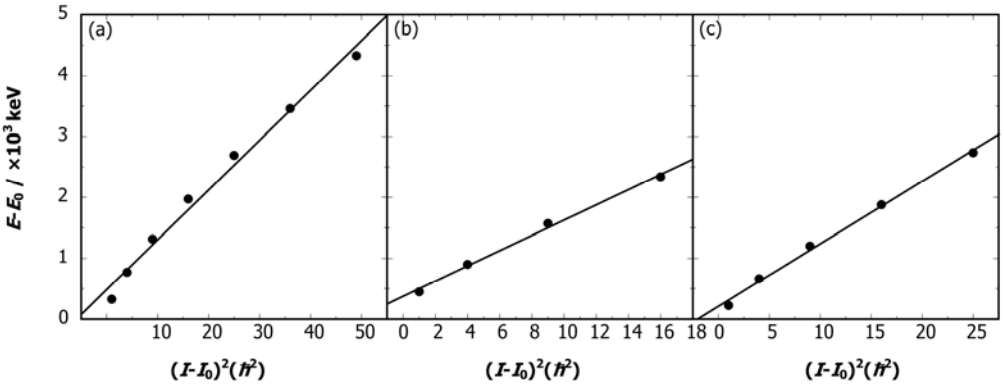

Fig.4 Relative energy (E) versus spin (I) curve for (a) band C, (b) band D and (c) band E, respectively. E_0 and I_0 are the bandhead energy and spin, respectively. The fitted curves are shown by the solid lines (see text for details).

In the present work, the features of the three dipole bands shown in Figs.1, 2 and 3 are compared with the general criteria of a MR band in which the level energies (E) and the spins (I) follow the pattern:

$$E\text{-}E_0=A_0(I\text{-}I_0)^2 \qquad (7)$$

where E_0 and I_0 are the energy and spin of the band head, respectively, and A_0 is a constant. We plot E-E_0 versus $(I\text{-}I_0)^2$ in Figs.4a, 4b and 4c for bands C, D, and E, respectively. The solid lines in the figure are the fittings of the data using the relation in Eq.(7). The good agreement of the data with the fitted curve, as shown in Fig.4, indicates that bands C, D and E all follow the relation in Eq.(7). The dynamic moments of the inertia $J^{(2)}$ obtained for the three bands with:

$$J^{(2)}(\mathrm{I})\approx\frac{2\hbar^2}{\Delta E_\gamma(I)}=\frac{2\hbar^2}{E_\gamma(I+1)-E_\gamma(I)} \qquad (8)$$

where $E_\gamma(I)\equiv E_\gamma(I\rightarrow I-1)$, are within the typical value of $J^{(2)}$~10-25$\hbar^2$MeV^{-1} for an MR band. Therefore, one may conclude that each of the above three bands is most likely to be an MR band.

4 Conclusion

High-spin states in ^{84}Rb were populated in the reaction ^{18}O+^{70}Zn at the beam energy of 75 MeV. Three negative-parity M1 sequences have been observed in the doubly odd nucleus ^{84}Rb, which shows the characteristic feature of magnetic rotation such as

regular level spacings and large probability ratios, of the magnetic dipole (M1) transition to the electric quadrupole (E2) transition, B(M1)/B(E2). The order of the experimental states is well reproduced in the projected shell model calculations with the basis of the four-quasiparticle configuration of the type $\pi(\mathrm{fp}) \otimes \pi(\mathrm{g}_{9/2}^2) \otimes \nu(\mathrm{g}_{9/2})$.

References

1 Döring J, Ulrich D, Johns G D, *et al.* Phys Rev C, 1999, **59**: 71–81.

2 Schnare H, Schwengner R, Frauendorf S, *et al.* Phys Rev Lett, 1999, **82**: 4408–4411.

3 Schwengner R, Rainovski G, Schnare H, *et al.* Phys Rev C, 2002, **66**: 024310.

4 Schwengner R, Schnare H, Frauendorf S, *et al.* J Res Natl Inst Stan, 2000, **105**: 133–136.

5 Madokoro H, Meng J, Matsuzaki M, *et al.* Phys Rev C, 2000, **62**: 061301(R).

6 Petrovici A, Schmid K W, Radu O, *et al*. Eur Phys J A, 2006, **28**: 19–25.

7 Shen S F, Han G B, Wen S X, *et al.* Phys Rev C, 2010, **82**: 014306.

8 Krane K S, Steffen R M, Wheeler R M. Atom Data Nucl Data, 1973, **11**: 351–406.

9 Radford D C. Nucl Instrum Meth A, 1995, **361:** 297–305.

10 Frauendorf S. Nucl Phys A, 1993, **557**: 259c–276c.

11 Palit R, Sheikh J A, Sun Y. Phys Rev C, 2003, **67**: 014321.

12 Hara K, Sun Y. Nucl Phys A, 1991, **529**: 445–466.

13 Hara K, Sun Y. Nucl Phys A, 1991, **531**: 221–236.

14 Hara K, Sun Y. Nucl Phys A, 1992, **537**: 77–99.

15 Hara K, Sun Y. Int J Mod Phys E, 1995, **4**: 637–764.

16 Andersson C G, Hellström G, Leander G, *et al.* Nucl Phys A, 1978, **309**: 141–176.

17 Möller P, Nix J R, Myers W D, *et al.* Atom Data Nucl Data, 1995, **59**: 185–381.

18 Kang X Z, Shen S F, Gu J Z, *et al.* J Phys Soc Jpn, 2011, **80**: 044201.